

# Truly Privacy-Preserving Federated Analytics for Precision Medicine with Multiparty Homomorphic Encryption

David Froelicher<sup>1</sup>, Juan R. Troncoso-Pastoriza<sup>1</sup>, Jean Louis Raisaro<sup>2,3</sup>, Michel A. Cuendet<sup>4</sup>, Joao Sa Sousa<sup>1</sup>, Hyunghoon Cho<sup>5</sup>, Bonnie Berger<sup>5,6,7</sup>, Jacques Fellay<sup>2,8</sup>, and Jean-Pierre Hubaux<sup>1,\*</sup>

<sup>1</sup>Laboratory for Data Security, EPFL, Lausanne, Switzerland

<sup>2</sup>Precision Medicine Unit, Lausanne University Hospital, Lausanne, Switzerland

<sup>3</sup>Data Science Group, Lausanne University Hospital, Lausanne, Switzerland

<sup>4</sup>Precision Oncology Center, Lausanne University Hospital, Lausanne, Switzerland

<sup>5</sup>Broad Institute of MIT and Harvard, Cambridge, Massachusetts, USA

<sup>6</sup>Computer Science and AI Laboratory, MIT, Cambridge, Massachusetts, USA

<sup>7</sup>Department of Mathematics, MIT, Cambridge, Massachusetts, USA

<sup>8</sup>School of Life Sciences, EPFL, Lausanne, Switzerland

\*jean-pierre.hubaux@epfl.ch

## ABSTRACT

Using real-world evidence in biomedical research, an indispensable complement to clinical trials, requires access to large quantities of patient data that are typically held separately by multiple healthcare institutions. Centralizing those data for a study is often infeasible due to privacy and security concerns. Federated analytics is rapidly emerging as a solution for enabling joint analyses of distributed medical data across a group of institutions, without sharing patient-level data. However, existing approaches either provide only limited protection of patients' privacy by requiring the institutions to share intermediate results, which can in turn leak sensitive patient-level information, or they sacrifice the accuracy of results by adding noise to the data to mitigate potential leakage. We propose FAMHE, a novel federated analytics system that, based on multiparty homomorphic encryption (MHE), enables privacy-preserving analyses of distributed datasets by yielding highly accurate results without revealing any intermediate data. We demonstrate the applicability of FAMHE to essential biomedical analysis tasks, including Kaplan-Meier survival analysis in oncology and genome-wide association studies in medical genetics. Using our system, we accurately and efficiently reproduce two published centralized studies in a federated setting, enabling biomedical insights that are not possible from individual institutions alone. Our work represents a necessary key step towards overcoming the privacy hurdle in enabling multi-centric scientific collaborations.

## 1 Introduction

2 A key requirement for fully realizing the potential of precision medicine is to make large amounts of medical data inter-operable  
3 and widely accessible to researchers. Today, however, medical data are scattered across many institutions, which renders  
4 centralized access and aggregation of such data extremely challenging, if not impossible. The challenges are not due to the  
5 technical hurdles of transporting high volumes of heterogeneous data across organizations but to the legal and regulatory  
6 barriers that make transfer of patient-level data outside a healthcare provider extremely complex and time-consuming. Moreover,  
7 stringent data-protection and privacy regulations (e.g., GDPR<sup>1</sup>) strongly restrict the transfer of personal data, including even  
8 pseudonymized data, across jurisdictions.

9 *Federated analytics* (FA) is emerging as a new paradigm that seeks to address the data governance and privacy issues related  
10 to medical-data sharing<sup>2-4</sup>. FA enables different healthcare providers to collaboratively perform statistical analyses and to  
11 develop machine-learning models, without exchanging the underlying datasets. Only aggregated results or model updates are  
12 transferred. In this way, each healthcare provider can define its own data governance and maintain control over the access  
13 to its patient-level data. FA offers unprecedented opportunities for exploiting large and diverse volumes of data distributed  
14 across multiple institutions. These opportunities can facilitate the development and validation of AI algorithms that yield more  
15 accurate, unbiased, and generalizable clinical recommendations, as well as accelerate novel discoveries. Such advances are  
16 particularly important in the context of rare diseases or medical conditions, where the number of affected patients in a single

17 institution is often not sufficient to identify meaningful statistical patterns with enough statistical power.

18 The adoption of FA in the medical sector, despite its potential, has been slower than expected. This is in large part due to  
19 the unresolved privacy issues of FA, related to the sharing of model updates or partial data aggregates in cleartext. Indeed,  
20 despite patient-level data not being transferred between the institutions engaging in FA, it has been shown that the model  
21 updates (or partial aggregates) themselves can, under certain circumstances, leak sensitive personal information about the  
22 underlying individuals, thus leading to re-identification, membership inference, and feature reconstruction<sup>5,6</sup>. Our work focuses  
23 on overcoming this key limitation of existing FA approaches. We note that limited data inter-operability across different  
24 healthcare providers is another potential challenge in deploying FA; this, in practice, can be surmounted by harmonizing the  
25 data across institutions before performing the analysis.

26 Several open-source software platforms have recently been developed to provide users streamlined access to FA algo-  
27 rithms<sup>3,7,8</sup>. For example, DataSHIELD<sup>7</sup> is a distributed data analysis and a machine-learning (ML) platform based on the  
28 open-source software R. However, none of these platforms address the aforementioned problem of indirect privacy leakages  
29 that stem from their use of ‘vanilla’ federated learning. Hence, it remains unclear whether these existing solutions are able to  
30 substantially simplify regulatory compliance, compared to more conventional workflows that centralize the data<sup>9–11</sup>, if the  
31 partial aggregates and model updates could still be considered as personal identifying data<sup>5,12–15</sup>.

32 More sophisticated solutions for FA, which aim to provide end-to-end privacy protection, including for the shared  
33 intermediate data, have been proposed<sup>16–25</sup>. These solutions use techniques such as differential privacy (diffP)<sup>26</sup>, secure  
34 multiparty computation (SMC), and homomorphic encryption (HE). However, these techniques often achieve stronger privacy  
35 protection at the expense of accuracy or computational efficiency, thus limiting their applicability. Existing diffP techniques for  
36 FA, which prevent privacy leakage from the intermediate data by adding noise to it before sharing, often require prohibitive  
37 amounts of noise, which leads to inaccurate models. Furthermore, there is a lack of consensus around how to set the privacy  
38 parameters for diffP in order to provide acceptable mitigation of inference risks in practice<sup>27</sup>. SMC and HE are cryptographic  
39 frameworks for securely performing computation over private datasets (pooled from multiple parties in the context of FA, in  
40 an encrypted form) without any intermediate leakage, but both come with notable drawbacks. SMC incurs a high network-  
41 communication overhead and has difficulty scaling to a large number of data providers. HE imposes high storage and  
42 computational overheads and introduces a single point of failure in the standard centralized setup, where a single party receives  
43 all encrypted datasets to securely perform the joint computation. Distributed solutions based on HE<sup>22–24,28</sup> have also been  
44 proposed to decentralize both the computational burden and the trust, but existing solutions address only simple calculations  
45 (e.g., counts and basic sample statistics) and are not suited for complex tasks.

46 Here, we present FAMHE, a new approach, based on multiparty homomorphic encryption (MHE)<sup>29</sup>, to privacy-preserving  
47 federated analytics, and we demonstrate its ability to enable an efficient federated execution of two fundamental workflows  
48 in biomedical research: Kaplan-Meier survival analysis and genome-wide association studies (GWAS). MHE is a recently  
49 proposed multiparty computation framework based on HE; it combines the power of HE to perform computation on encrypted  
50 data without communication between the parties, with the benefits of interactive protocols, which can greatly simplify certain  
51 expensive HE operations. Building upon the MHE framework, we introduce a novel approach to FA, where each participating  
52 institution performs local computation and encrypts the intermediate results by using MHE; the results are then combined  
53 (e.g., aggregated) and distributed back to each institution for further computation. This process is repeated until the desired  
54 analysis is completed. Contrary to diffP-based approaches that rely on obfuscation techniques to mitigate the leakage in  
55 intermediate results, by sharing only encrypted intermediate results, FAMHE provides end-to-end privacy protection, without  
56 sacrificing accuracy. By sharing only encrypted information, our approach guarantees that, whenever needed, a minimum level  
57 of obfuscation can be applied only to the final result in order to protect it from inference attacks, instead of being applied to all  
58 intermediate results. Furthermore, FAMHE improves over both SMC and HE approaches by minimizing communication, by  
59 scaling to large numbers of data providers, and by circumventing expensive non-interactive operations (e.g., bootstrapping in  
60 HE). Our work also introduces a range of optimization techniques for FAMHE, including optimization of the local vs. collective  
61 computation balance, ciphertext packing strategies, and polynomial approximation of complex operations; these techniques are  
62 instrumental in our efficient design of FAMHE solutions for survival analysis and GWAS.

63 We demonstrate the performance of FAMHE by replicating two published multi-centric studies that originally relied on data  
64 centralization. These include a study of metastatic cancer patients and their tumor mutational burden<sup>30</sup>, and a host genetic study  
65 of HIV-1 infected patients<sup>31</sup>. By distributing each dataset across multiple data providers and by performing federated analyses  
66 using our approach, we successfully recapitulated the results of both original studies. Our solutions are efficient in terms of both  
67 execution time and communication, e.g., completing a GWAS over 20K patients and four million variants in less than five hours.  
68 In contrast to most prior work on biomedical FA, which relied on artificial datasets<sup>16,18,24,32</sup>, our results closely reflect the  
69 potential of our approach in real application settings. Furthermore, our approach has the potential to simplify the requirements  
70 for contractual agreements and the obligations of data controllers that often hinder multi-centric medical studies, because data  
71 processed by using MHE can be considered anonymous data under the General Data-Protection Regulation (GDPR)<sup>12</sup>. Our

72 work shows that FAMHE is a practical framework for privacy-preserving FA for biomedical workflows and it has the power to  
73 enable a range of analyses beyond those demonstrated in this work.

## 74 Results

### 75 Overview of FAMHE

76 In FAMHE, we rely on MHE to perform privacy-preserving FA by pooling the advantages of both interactive protocols and  
77 HE and by minimizing their disadvantages. In particular, by relying on MHE and on the distributed protocols for federated  
78 analytics proposed by Froelicher et al.<sup>25</sup>, our approach enables several sites to compute on their local patient-level data and  
79 then encrypt (*Local Computation & Encryption* in Figure 1) and homomorphically combine their local results under MHE  
80 (*Collective Aggregation* in Figure 1). These local and global steps can be repeated (*Iterate* in Figure 1), depending on the  
81 analytic task. At each new iteration, participating sites use the encrypted combination of the results of the previous iteration to  
82 compute on their local data without the need for decryption, e.g., gradient descent steps in the training of a regression model.  
83 The collectively encrypted and aggregated final result is eventually switched (*Collective Key Switching* in Figure 1) from an  
84 encryption under the collective public key to an encryption under the querier's public key (the blue lock in Figure 1) such that  
85 only the querier can decrypt. The use of MHE ensures that the secret key of the underlying HE scheme never exists in full.  
86 Instead, the control over the decryption process is distributed across all participating sites, each one holding a fragment of the  
87 decryption key. This means that all participating sites have to agree to enable the decryption of any piece of data, and that no  
88 single entity alone can decrypt the data. As described in *System and Threat Model* in *Online Methods*, FAMHE is secure in a  
89 passive adversarial model in which all-but-one data providers can be dishonest and collude among themselves.

90 FAMHE builds upon novel optimization techniques for enabling the efficient execution of complex iterative workflows: (1)  
91 by relying on edge-computing and optimizing the use of computations on the data providers' cleartext data; (2) by relying on the  
92 packing ability of the MHE scheme to encrypt a vector of values in a single ciphertext such that any computation on a ciphertext  
93 is performed simultaneously on all the vector values, i.e., Single Instruction, Multiple Data (SIMD); (3) by further building on  
94 this packing property to optimize the sequence of operations by formatting a computation output correctly for the next operation;  
95 (4) by approximating complex computations such as matrix inversion (i.e., division) by polynomial functions (additions and  
96 multiplications) to efficiently compute them under HE; and (5) by replacing expensive cryptographic operations by lightweight  
97 interactive protocols. Note that FAMHE avoids the use of centralized complex cryptographic operations that would require a  
98 much more conservative parameterization and would result in higher computational and communication overheads (e.g., due to  
99 the use of larger ciphertexts). Therefore, FAMHE efficiently minimizes the computation and communication costs for a high  
100 security level. We provide more details of our techniques in *Online Methods*.

101 We implemented FAMHE based on Lattigo<sup>33</sup>, an open-source Go library for multiparty lattice-based homomorphic encryption  
102 (MHE) cryptography. We chose the security parameters to always ensure a high 128-bit-level security. We refer to *Online*  
103 *Methods* for a detailed configuration of FAMHE used in our experiments.

104 To demonstrate the performance of FAMHE, we developed efficient federated-analytics solutions based on FAMHE and our  
105 optimization techniques for two essential biomedical tasks: Kaplan-Meier survival analysis and GWAS (*Online Methods*).  
106 We present the results of these solutions on real datasets from two peer-reviewed studies that were originally conducted by  
107 centralizing the data from multiple institutions.

### 108 Multi-centric Kaplan-Meier Survival Analysis Using FAMHE

109 Kaplan-Meier survival analysis is a widely used method to assess patients' response (i.e., survival) over time to a specific  
110 treatment. For example, in a recent study, Samstein et al.<sup>30</sup> demonstrated that the tumor mutational burden (TMB) is a predictor  
111 of clinical responses to immune checkpoint inhibitor (ICI) treatments in patients with metastatic cancers. To obtain this  
112 conclusion, they computed Kaplan-Meier overall survival (OS) curves of 1,662 advanced-cancer patients treated with ICI and  
113 that are stratified by TMB values. OS was measured from the date of first ICI treatment to time of death or the last follow-up.  
114 In Figure 2a, we show the survival curves obtained from the original centralized study (*Centralized, Non-secure*) and those  
115 obtained through our privacy-preserving federated workflow of FAMHE executed among three data providers (DPs). Note that  
116 for FAMHE, to illustrate the workflow of federated collaboration, we distributed the dataset across the DPs, each hosted on  
117 a different machine. FAMHE's analysis is then performed with each DP having access only to the locally held patient-level  
118 data, thus closely reflecting a real collaboration setting that involves independent healthcare centers. As a result, our federated  
119 solutions circumvent the privacy risks associated with data centralization in the original study. We observed that FAMHE  
120 produces survival curves identical to those of the original non-secure approach. By using either approach, we are able to derive  
121 the key conclusion that the benefits of ICI increase with TMB.

122 In Figure 2b, we show that FAMHE produces exact results while maintaining computational efficiency, as the computation of  
123 the survival curves shown in Figure 2a is executed in less than 12 seconds, even when the data are scattered among 96 DPs. We  
124 also observe that the execution time is almost independent of the DPs' dataset size, as the same experiment performed on a 10x

125 larger dataset (replicated 10x) takes almost exactly the same amount of time. We show that FAMHE's execution time remains  
126 below 12 seconds for up to 8192 time points. We note that, in this particular study, the number of time points (instants at which  
127 an event can occur) is smaller than 200, due to the rounding off of survival times to months. In summary, the FAMHE-based  
128 Kaplan-Meier estimator produces precise results and scales efficiently with the number of time points, each DPs' dataset size,  
129 and with the number of DPs. We remark that the hazard ratio, which is often computed in survival curve studies, can be directly  
130 estimated by the querier, based on the final result<sup>34</sup>. It is also possible to compute the hazard ratios directly by following the  
131 general workflow of FAMHE described in Figure 1. This requires the training of proportional hazard regression models that are  
132 closely related to generalized linear models<sup>35</sup> that our GWAS solution also utilizes.

### 133 Multi-centric Genome-Wide Association Studies Using FAMHE

134 Genome-wide association studies (GWAS) are a fundamental analysis tool in medical genetics that identifies genetic variants  
135 that are statistically associated with given traits, such as disease status. GWAS have led to numerous discoveries about human  
136 health and biology, and efforts to collect larger and more diverse cohorts to improve the power of GWAS. Their relevance to  
137 diverse human populations continue to grow. As we progress toward precision medicine and genetic sequencing becomes  
138 more broadly incorporated into routine patient care, large-scale GWAS that span multiple medical institutions will become  
139 increasingly more valuable. Here we demonstrate the potential of FAMHE to enable multi-centric GWAS that fully protect the  
140 privacy of patients' data throughout the analysis.

141 We evaluated our approach on a GWAS dataset from McLaren et al.<sup>31</sup>; they studied the host genetic determinants of HIV-1  
142 viral load in an infected population of European individuals. It is known that the viral load observed in an asymptomatic patient  
143 after primary infection positively correlates with the rate of disease progression; this is the basis for the study of how host  
144 genetics modulates this phenotype. We obtained the available data for a subset of the cohort including 1,857 individuals from  
145 the Swiss HIV Cohort Study, with 4,057,178 genotyped variants. The dataset also included 12 covariates that represent ancestry  
146 components, which we also used in our experiments to correct for confounding effects. To test our federated analysis approach,  
147 we distributed, in a manner analogous to the survival analysis experiments, the GWAS dataset across varying numbers of data  
148 providers.

149 Following the approach of McLaren et al.<sup>31</sup>, we performed GWAS using linear regression of the HIV-1 viral load on each  
150 of the more than four million variants, always including the covariates. To enable this large-scale analysis in a secure and  
151 federated manner, we developed two complementary approaches based on our system: FAMHE-GWAS and FAMHE-FastGWAS.  
152 FAMHE-GWAS performs exact linear regression and incurs no loss of accuracy, whereas FAMHE-FastGWAS achieves faster  
153 runtime through iterative optimization at a small expense of accuracy. We believe that both modes are practical and that the  
154 choice between them would depend on the study setting. Importantly, both solutions do not reveal intermediate results at any  
155 point during the computation, and any data exchanged between the data providers (DPs) to facilitate the computation are always  
156 kept hidden by collective encryption. We also emphasize that the DPs in both solutions utilize their local cleartext data and  
157 securely aggregate encrypted intermediate results, following the workflow presented in Figure 1.

158 Both our solutions use a range of optimized computational routines that we developed in this work to carry out the  
159 sophisticated operations required in GWAS by using multiparty homomorphic encryption (MHE). In FAMHE-GWAS, we exploit  
160 the fact that the same set of covariates are included in all regression models by computing once the inverse covariance matrix of  
161 the covariates, then for each variant computing an efficient update to the inverse matrix to reflect the contribution of each given  
162 variant. Our solution employs efficient MHE routines for each of these steps, including matrix inversion. In FAMHE-FastGWAS,  
163 we first subtract the covariate contributions from the phenotype by training once a linear model including only the covariates.  
164 We then train in parallel uni-variate models for all four million variants. We perform this step efficiently by using the stochastic  
165 gradient descent algorithm implemented with MHE. Taken together, these techniques illustrate the computational flexibility of  
166 FAMHE and its potential to enable a wide range of analyses. Further details of our solutions are provided in *Online Methods*.

167 We compare FAMHE-GWAS and FAMHE-FastGWAS against (i) *Original*, the centralized non-secure approach adopted by  
168 the original study, albeit on the Swiss HIV Cohort Study dataset, (ii) *Meta-analysis*<sup>36</sup>, a solution in which each DP locally  
169 and independently performs GWAS to obtain summary statistics that are then shared and combined (through weighted-Z test)  
170 across DPs to produce a single statistic for each variant that represents its overall association with the target phenotype, and (iii)  
171 *Independent*, a solution in which a data provider uses only its part of the dataset to perform GWAS. For all baseline approaches,  
172 we used the PLINK<sup>36</sup> software to perform the analysis (see *Online Methods* for the detailed procedure). Note that *Meta-analysis*  
173 can also be securely executed by first encrypting each DP's local summary statistics then following the federated-analytics  
174 workflow presented in Figure 1.

175 The Manhattan plots visualizing the GWAS results obtained by each method are shown in Figure 3a. Both our FAMHE-based  
176 methods produced highly accurate outputs that are nearly indistinguishable from the *Original* results. Consequently, our  
177 methods successfully implicated the same genomic regions with genome-wide significance found by *Original*, represented by  
178 the strongest associated SNPs rs7637813 on chromosome 3 (nominal  $p = 7.2 \times 10^{-8}$ ) and rs112243036 on chromosome 6

( $p = 7.0 \times 10^{-21}$ ). Notably, both these SNPs are in close vicinity to the two strongest signals reported by the original study<sup>31</sup>: rs1015164 at a distance of 9 Kbp and rs59440261 at a distance of 42 Kbp, respectively. The former is found in the major histocompatibility complex (MHC) region, and the latter is near the *CCR5* gene; both have established connections to HIV-1 disease progression<sup>31</sup>. Although the two previous SNPs were not available in our data subset to be analyzed, we reasonably posit that our findings capture the same association signals as in the original study, related through linkage disequilibrium. Regardless, we emphasize that our federated analysis results closely replicated the centralized analysis of the same dataset we used in our analysis.

In contrast, the *Meta-analysis* approach, though successfully applied in many studies, severely underperformed in our experiments by reporting numerous associations that are likely spurious. We believe this observation highlights the limitation of meta-analyses when the sample sizes of individual datasets are limited. Similarly, the *Independent* approach obtained noisy results, which was further compounded by the issue of limited statistical power (for results obtained by every data provider, see *Supplementary Figure S4*). We complement these comparisons with Table 1 that quantifies the error in the reported negative logarithm of p-value ( $-\log_{10}(P\text{-val})$ ), as well as the regression weights ( $w$ ), for all of the considered approaches compared to *Original*. We observed that FAMHE-FastGWAS yields an average absolute error always smaller than  $10^{-2}$ , which ensures accurate identification of association signals. FAMHE-GWAS further reduces the error by roughly a factor of three to obtain even more accurate results. Whereas, *Meta-analysis* and *Independent* approaches result in considerably larger errors.

FAMHE scales efficiently in all dimensions: number of data providers, samples and variants (Figure 4). As displayed by Figure 4a, FAMHE's runtime decreases when the workload is distributed among more data providers, and it is below one hour for a GWAS jointly performed by 12 data providers on more than 4 million variants with FAMHE-FastGWAS. It also shows that in a wide-area network (WAN) where the bandwidth is halved (from 1Gbps to 500Mbps) and the delay doubled (from 20ms to 40ms), FAMHE execution time increases by a maximum of 26% over all experiments. FAMHE's execution time grows linearly with the number of patients (or samples) and variants (Figures 4c and 4b). In all experiments, the communication accounts for between 4 and 55 percent of FAMHE total execution time. As described in *Online Methods*, FAMHE computes the p-values of multiple (between 512 and 8192) variants in parallel, due to the *Single Instruction, Multiple Data (SIMD)* property of the cryptoscheme and is further parallelized among the DPs and by multi-threading at each DP. FAMHE is therefore highly parallelizable, i.e., doubling the number of available threads would almost halve the execution time. Finally, FAMHE-GWAS, which performs exact linear regression, further reduces the error (by a factor of 3x compared to FAMHE-FastGWAS), but its execution times are generally higher than FAMHE-FastGWAS.

These results demonstrate the ability of FAMHE to enable the execution of FA workflows on data held by large numbers of data providers who keep their data locally, while allowing full privacy with no loss of accuracy. To our knowledge, no other existing approaches achieve all of these properties: The FA approaches that share intermediate analysis results in cleartext among the data providers offer limited privacy-protection or, when used together with diffP techniques to mitigate leakage, they sacrifice accuracy. Meta-analysis approaches yield imprecise results compared to joint analysis, especially in settings where each DP has access to small cohorts, as we have shown. According to our estimates, centralized HE-based solutions have execution times that are 1-3 orders of magnitude greater than FAMHE due to the overhead of centralized computation, as well as compute-intensive cryptographic operations required by centralized HE (e.g., bootstrapping). Finally, SMC approaches, though an alternative for a small network of 2-4 data providers, have difficulty supporting a large number of DPs, due to their high communication overhead. Note that communication of SMC scales with the combined size of all datasets, whereas FAMHE shares only aggregate-level data, thus vastly reducing the communication burden. We provide a more detailed discussion of existing solutions and estimates of their computational costs in *Supplementary Note 4*.

## Discussion

Here, we have demonstrated that efficient privacy-preserving federated-analysis workflows for complex biomedical tasks are attainable. Our efficient solutions for survival analysis and GWAS, based on our new paradigm FAMHE, accurately reproduced published peer-reviewed studies while keeping the dataset distributed across multiple sites and ensuring that the shared intermediate-data do not leak any private information. Alternative approaches based on meta-analysis or independent analysis of each data set led to noisy results in our experiments, illustrating the benefits of our federated solutions. The fact that FAMHE led to practical federated algorithms for both the statistical calculations required by Kaplan-Meier curves and the large-scale regression tasks of GWAS reflects the ability of FAMHE to enable a wide range of other analyses in biomedical research, such as cohort exploration and the training and evaluation of disease risk prediction models.

Conceptually, FAMHE represents a novel approach to federated analytics; it has not been previously explored for complex biomedical tasks. FAMHE combines the strengths of both conventional federated-learning approaches and cryptographic frameworks for secure computation. Like federated learning, FAMHE scales to large numbers of data providers and enables non-interactive local computation over each institution's dataset (available locally in cleartext), which approach minimizes the computational and communication burdens that cryptographic solutions<sup>18,19,22-24,37</sup> typically suffer from. However, FAMHE

233 draws from the cryptographic framework of MHE to enable secure aggregation and local computation of intermediate results  
234 in an encrypted form. This approach departs from the existing federated learning solutions<sup>2,3,7,16,17,21</sup> that largely rely on  
235 data obfuscation to mitigate leakage in the intermediate data shared among the institutions. Our approach thus provides more  
236 rigorous privacy protection. In other words, in FAMHE, accuracy is traded off only with performance, similarly to non-secure  
237 federated approaches, but differently from obfuscation-based solutions, FAMHE's security is absolute. We summarize our  
238 comparison of FAMHE with existing works in Supplementary Table S1, *Supplementary Note 4*, and we refer to *Online Methods*  
239 for more details.

240 The fact that FAMHE shares only encrypted data among the data providers has important implications for its suitability to  
241 regulatory compliance and its potential to catalyze future efforts for multi-centric biomedical studies. In recent work, it has  
242 been established by privacy law experts that data processed using MHE can be considered 'anonymous' data under the General  
243 Data Protection Regulation (GDPR)<sup>12</sup>. Anonymous data, which refers to data that require unreasonable efforts to re-identify the  
244 source individuals, lies outside the jurisdiction of GDPR. Therefore, our approach has the potential to significantly simplify the  
245 requirements for contractual agreements and the obligations of data controllers with respect to regulations, such as GDPR, that  
246 often hinder multi-centric medical studies. In contrast, existing federated-analytics solutions, where the intermediate results are  
247 openly shared, present more complicated paths toward compliance, as intermediate results could still be considered personal  
248 data<sup>13-15</sup>.

249 In cases where the potential leakage of privacy in the final output of federated analysis is a concern, differential privacy  
250 techniques can be easily incorporated into FAMHE by adding a small perturbation to the final results before they are revealed. In  
251 contrast to the conventional federated learning approach, which requires each data provider to perturb its local results before  
252 aggregating them with other parties, FAMHE enables the data providers to keep the local results encrypted and reveals only the  
253 final aggregated results. Therefore, FAMHE can use a smaller amount of added noise and achieve the same level of privacy<sup>38</sup>.  
254 Notably, the choices of differential-privacy parameters suitable for analyses with a high-dimensional output, such as GWAS,  
255 can be challenging and needs to be further explored.

256 There are several directions in which our work could be extended to facilitate the adoption of FAMHE. Although we  
257 reproduced published studies by distributing a pooled dataset across a group of data providers, jointly analyzing multiple  
258 datasets by using FAMHE that could not be combined otherwise would be a challenging yet important milestone for this  
259 endeavour. Our work demonstrates FAMHE's applicability on a reliable baseline and constitutes an important and necessary step  
260 towards building trust in our technology and fostering its adoption, thus enabling its use for the discovery of new scientific  
261 insights. Furthermore, we will extend the capabilities of FAMHE by developing additional protocols for a broader range of  
262 standard analysis tools and machine-learning algorithms in biomedical research (e.g., proportional-hazard regression models). A  
263 key step in this direction is to make our implementation of FAMHE easily configurable by practitioners for their own applications.  
264 Specifically, connecting FAMHE to existing user-friendly platforms such as MedCo<sup>39</sup> to make it widely available would help  
265 empower the increasing efforts to launch multi-centric medical studies and accelerate scientific discoveries.

## 266 Online Methods

267 Here, we describe the crypto-scheme that we rely on to build FAMHE and discuss how FAMHE differs from existing work. We  
268 describe FAMHE's system and threat model, before detailing the execution of the privacy-preserving pipelines for survival  
269 curves and GWAS studies. Finally, we detail our experimental settings and explain how differential privacy can be ensured on  
270 the final result in FAMHE.

## 271 Cryptographic Background

272 In FAMHE, the data exchanged by the data providers are always encrypted such that only the querier can decrypt the final  
273 result. For this purpose, we rely on a multiparty (or distributed) fully-homomorphic encryption scheme<sup>29</sup> in which the secret  
274 key is distributed among the parties and the corresponding collective public key  $pk$  is publicly known. Thus, each party can  
275 independently compute on ciphertexts encrypted under  $pk$  (the yellow lock in Figure 1), but all parties have to collaborate to  
276 decrypt a ciphertext. Hence, as long as one data provider (DP) is honest and refuses to participate in the decryption, encrypted  
277 data cannot be decrypted. This multiparty scheme also enables DPs to collectively switch the encryption key of a ciphertext  
278 from  $pk$  to another public key, i.e., the querier's key (blue lock), without decrypting. We provide a list of recurrent symbols in  
279 *Supplementary Table S3*. Mouchet et al.<sup>29</sup> propose a multiparty version of the Brakerski Fan-Vercauteren (BFV) lattice-based  
280 homomorphic cryptosystem<sup>40</sup> and introduce interactive protocols for key management and cryptographic operations. We rely  
281 directly on this multiparty scheme for the computation of Kaplan-Meier survival curves, which involves only exact integer  
282 arithmetic, and we use an adaptation to the Cheon-Kim-Kim-Song cryptosystem (CKKS)<sup>41</sup> (described by Froelicher et al.<sup>25</sup>)  
283 that enables approximate arithmetic for the GWAS operations. Froelicher et al.<sup>25</sup> showed that this adaptation satisfies similar  
284 security properties to the original scheme proposed by Mouchet et al.<sup>29</sup>. The security comes mainly from the fact that the  
285 underlying (centralized) cryptoschemes, i.e., BFV and CKKS, share the same computational assumptions and are based on the

286 same hard problem, i.e., the decisional RLWE problem<sup>42</sup>. In *Novel Optimization Techniques*, we discuss the SIMD property of  
287 these cryptosystems and how FAMHE builds on it to efficiently execute FA workflows with encrypted data.

## 288 Related Work

289 Centralized solutions for medical-data sharing<sup>9–11</sup> require large amounts of data to be stored in a single repository that becomes  
290 a single point of failure and that (often) has to be fully trusted.

291 To alleviate this trust assumption, federated-learning solutions<sup>2,3,7</sup> were proposed. In these solutions, the data providers  
292 keep their data locally and share only aggregates or training-model updates with a central server. However, multiple research  
293 contributions<sup>13–15</sup> have shown that these aggregates can still reveal significant information about the data providers' data. For  
294 example, Nasirigerdeh et al. proposed sPLINK<sup>3</sup>, a federated instantiation of the PLINK<sup>36</sup> software to perform a GWAS. With  
295 sPLINK the data providers' partial covariance matrices (i.e., intermediate result) are revealed to the server that aggregates these  
296 matrices in order to perform the models training. Although the original data  $X$  is not actually transferred, some information  
297 about the original data can be inferred from the covariance matrix  $X^T X$  computed by the aggregating server. In FAMHE, the  
298 covariance matrix is collectively and obliviously computed by exchanging encrypted data such that the models can be trained  
299 without revealing any intermediate data.

300 Similarly, secure multiparty solutions<sup>18,19</sup> rely on secret-sharing to compute on medical data without revealing intermediate  
301 or aggregate information. Cho et al.<sup>19</sup> designed a three-party secret-sharing-based solution for enabling GWAS execution while  
302 not revealing information on the input data. Secret-sharing-based solutions require the data providers to communicate their data  
303 to a limited number of computing nodes, i.e., outside their premises. FAMHE efficiently scales to federated learning settings  
304 where many DPs locally keep their data.

305 Distributed solutions relying on homomorphic encryption<sup>22–24,37</sup> to enable federated analytics in a trust model similar to  
306 FAMHE were proposed. Some of these works assume a threat model more constraining than FAMHE, as they consider an active  
307 malicious adversary, but also exclusively focus on simple computations, e.g., counts and simple statistics. To propose a generic  
308 federated workflow for biomedical federated analytics, we build on the multiparty homomorphic encryption-based protocols  
309 proposed by Froelicher et al.<sup>25</sup>. We show how the sophisticated GWAS computation can be efficiently performed through this  
310 workflow.

311 Differential-privacy-based solutions<sup>16,17,21</sup>, in which the intermediate values are obfuscated by a specific amount of noise,  
312 assume a paradigm different than FAMHE, as privacy is traded off with accuracy. In fact, this obfuscation decreases the data and  
313 model utility. The training of accurate models requires high-privacy budgets, but the achieved privacy level remains unclear<sup>27</sup>.  
314 In FAMHE, similarly to standard cleartext non-secure solutions (e.g., PLINK<sup>36</sup>), the accuracy is traded for only the performance.  
315 We show in *Results* that FAMHE achieves an accuracy similar to standard non-secure solutions, and that it is able to scale to a  
316 high number of data providers and yields an acceptable execution time.

## 317 System & Threat Model

318 FAMHE supports a network of mutually distrustful medical institutions that act as data providers (DPs) and hold subjects'  
319 records. An authorized querier (see Figure 1) can run queries, without threatening the data confidentiality and subjects' privacy.  
320 The DPs and the querier are assumed to follow the protocol and to provide correct inputs. All-but-one data providers can be  
321 dishonest, i.e., they can try to infer information about other data providers by using the protocol's outputs. We assume that the  
322 DPs are available during the complete execution of a computation. However, to account for unresponsive DPs, FAMHE can use  
323 a threshold-encryption scheme, where the DPs secret-share<sup>43</sup> their secret keys, thus enabling a subset of the DPs to perform the  
324 cryptographic interactive protocols.

325 FAMHE can be extended to withstand malicious behaviors. A malicious data provider can try to disrupt the federated  
326 collaboration process, i.e., by performing wrong computations or inputting wrong results. This can be partially mitigated  
327 by requiring the DPs to publish transcripts of their computations and to produce zero-knowledge proofs of range<sup>44</sup>, thus  
328 constraining the DPs' possible inputs. Also, the querier can try to infer information about a DP's local data from the final result.  
329 FAMHE can mitigate this inference attack by limiting the number of requests that a querier can perform and by adding noise to  
330 the final result (see *Discussion*) to achieve differential privacy guarantees. Learning how to select the privacy parameters and to  
331 design a generic solution to apply these techniques for the wide-range of applications enabled by FAMHE is part of future work.

## 332 FAMHE's Novel Optimization Techniques

333 Here, we describe the main optimization techniques introduced in FAMHE. We will explain how these optimizations are used in  
334 FAMHE to compute survival curves and GWAS.

335 In order to parallelize and efficiently perform computationally-intensive tasks, we rely on the *Single Instruction, Multiple  
336 Data* (SIMD) property of the underlying cryptoscheme and on edge computing, i.e., the computations are pushed to the data  
337 providers. In MHE, a ciphertext encrypts a vector of  $N$  values and any operation (i.e., addition, multiplication, and rotation)  
338 performed on the ciphertext is executed on all the values simultaneously, i.e., SIMD. After a certain number of operations, the

339 ciphertext needs to be refreshed, i.e., bootstrapped. A rotation is, in terms of computation complexity, one order of magnitude  
 340 more expensive than an addition/multiplication; and a bootstrapping in a centralized setting is multiple orders of magnitudes  
 341 (2-4) more expensive than any other operation. As the security parameters determine how many operations can be performed  
 342 before a ciphertext needs to be bootstrapped, conservative parameters that incur large ciphertexts but enable more operations  
 343 without bootstrap are usually required in centralized settings. This results in higher communication and computation costs.  
 344 With MHE, a ciphertext can be refreshed by a lightweight interactive protocol that, besides its efficiency, also alleviates  
 345 the constraints on the cryptographic parameters and enables FAMHE to ensure a high level of security and still use smaller  
 346 ciphertexts. For example, we show in Figure 2b how FAMHE's execution time to compute a survival curve increases when  
 347 doubling the size of a ciphertext (from 4096 to 8192 slots).

348 As discussed in *Privacy-Preserving Pipeline for GWAS*, in the case of GWAS, FAMHE efficiently performs multiple  
 349 subsequent large-dimension matrix operations (*Supplementary Figure S2a*) by optimizing the data packing (*Supplementary*  
 350 *Figure S3*) to perform several multiplications in parallel and to minimize the amount of transformations required on the  
 351 ciphertexts. FAMHE builds on the data providers' ability to compute on their cleartext local data and combine them with  
 352 encrypted data, thus reducing the overall computation complexity. GWAS also requires non-polynomial functions, e.g., the  
 353 inverse of a matrix, to be evaluated on ciphertexts, which is not directly applicable in HE. In FAMHE, these non-polynomial  
 354 functions are efficiently approximated by relying on Chebyshev polynomials. We chose to rely on Chebyshev polynomials  
 355 instead of on least-square polynomial approximations in order to minimize the maximum approximation error hence avoid that  
 356 the function diverges on specific inputs. This technique has been shown to accurately approximate non-polynomial functions  
 357 in the training of generalized models<sup>25</sup> and neural networks<sup>45</sup>, which further shows the generality and applicability of our  
 358 proposed framework.

359 FAMHE combines the aforementioned features to efficiently perform FA with encrypted data. In GWAS, for example, we  
 360 rely on the Gauss-Jordan (GJ) method<sup>46</sup> to compute the inverse of the covariance matrix. We chose this algorithm as it can be  
 361 efficiently executed by relying on the aforementioned features: row operations can be efficiently parallelized with SIMD and  
 362 divisions are replaced by polynomial approximations.

### 363 Privacy-Preserving Pipeline for Survival Curves

364 Survival curves are generally estimated with the Kaplan-Meier estimator<sup>47</sup>

$$\hat{S}(t) = \prod_{j, t_j \leq T} \left( 1 - \frac{d_j}{n_j} \right), \quad (1)$$

365 where  $t_j$  is a time when at least one event has occurred,  $d_j$  is the number of events at time  $t_j$ , and  $n_j$  is the number of individuals  
 366 known to have survived (or at risk) just before the time point  $t_j$ . We show in Figure 2a the exact replica of the survival curve  
 367 presented by Samstein et al.<sup>30</sup> produced by our distributed and privacy-preserving computation. In a survival curve, each step  
 368 down is the occurrence of an event. The ticks indicate the presence of censored patients, i.e., patients who withdrew from the  
 369 study. The number of censored patients at time  $t_j$  is indicated by  $c_j$ . As shown in *Supplementary Figure S1*, to compute this  
 370 curve, each data provider  $i$  locally computes, encodes and encrypts a vector of the form  $n_0^{(i)}, c_0^{(i)}, d_0^{(i)}, \dots, n_T^{(i)}, c_T^{(i)}, d_T^{(i)}$  containing  
 371 the values  $n_j^{(i)}, c_j^{(i)}, d_j^{(i)}$  corresponding to each time point  $t_j$  for  $t_j = 0, \dots, T$ . All the DPs' vectors are then collectively aggregated.  
 372 The encryption of the final result is then collectively switched from the collective public key  $pk$  to the querier's public key that  
 373 can decrypt the result with its secret key and generate the curve following Eq. (1).

### 373 Privacy-Preserving Pipeline for GWAS

374 We briefly describe the genome-wide association-study workflow before explaining how we perform it in a federated and  
 375 privacy-preserving manner. We conclude by detailing how we obtained our baseline GWAS results in *Results* with the PLINK  
 376 software.

377 We consider a dataset of  $p$  samples, i.e., patients. Each patient is described by  $f$  features or covariates (with indexes 1 to  
 378  $f$ ). We list all recurrent symbols and acronyms in *Supplementary Table S3*. Hence, we have a covariates matrix  $X \in \mathbb{R}^{(p \times f)}$ .  
 379 Each patient also has a phenotype or label, i.e.,  $y \in \mathbb{R}^{(p \times 1)}$  and  $v$  variant values, i.e., one for each variant considered in the  
 380 association test. The  $v$  variant values for all  $p$  patients form another matrix  $V \in \mathbb{R}^{(p \times v)}$ . To perform the GWAS, for each variant  
 381  $i$ , the matrix  $X' = [1, X, V[:, i]] \in \mathbb{R}^{(p \times (f+2))}$ , i.e., the matrix  $X$  is augmented by a column of 1s (intercept) and the column of  
 382 one variant  $i$ , is constructed. The vector  $w \in \mathbb{R}^{(f+2)}$  is then obtained by  $w = (X'^T X')^{(-1)} X'^T y$ . The p-value for variant  $i$  is then  
 383 obtained with  $p_{val} = 2 \cdot pnorm(-|\frac{w[f+2]}{\sqrt{(MSE(y, y') \cdot (X'^T X')^{(-1)}[f+2, f+2])}}|)$  where  $pnorm$  is the cumulative distribution function (CDF)  
 384 of the standard normal distribution,  $w[f+2]$  is the weight corresponding to the variant,  $MSE(y, y')$  is the mean squared error

385 obtained from the prediction  $y'$  computed with  $w$ , and  $(X^T X')^{(-1)}[f+2; f+2]$  corresponds to the standard error of the variant  
386 weight.

387 Although this computation has to be performed for each variant  $i$ , we remark that  $X$  is common to all variants. In order  
388 to compute  $(X^T X)^{(-1)}$  only once before adjusting it for each variant and thus obtain  $(X^T X')^{(-1)}$ , we rely on the Sherman-  
389 Morrison formula<sup>48</sup> and the method presented in the report on cryptographic and privacy-preserving primitives (page 52) of the  
390 WITDOM European project<sup>49</sup>. We describe this approach, i.e., FAMHE-GWAS, in *Supplementary Protocol S2a*. Each data  
391 provider  $DP_i$  has a subset of  $p_i$  patients. For efficiency, the DPs are organized in a tree structure and one DP is chosen as the  
392 root of the tree  $DP_R$ . We remark that, as any exchanged information is collectively encrypted, this does not have any security  
393 implications. In a *Collective Aggregation (CA)*, each DP encrypts  $(E())$  its local result with the collective key, aggregates its  
394 children DPs encrypted results with its encrypted local results, and sends the sum to its parent DP such that  $DP_R$  obtains the  
395 encrypted result aggregated among all DPs. We recall here that with the homomorphic-encryption scheme used, vectors of  
396 values can be encrypted in one ciphertext and that any operation performed on a ciphertext is simultaneously performed on all  
397 vector elements, i.e., *Single Instruction, Multiple Data (SIMD)*. We rely on this property to parallelize the operations at multiple  
398 levels: among the DPs, among the threads in each DP and among the values in the ciphertexts.

399 We rely on the Gauss-Jordan (GJ) method<sup>46</sup> to compute the inverse of the encrypted covariance matrix. We chose this  
400 algorithm as it requires only row operations, which can be efficiently performed with SIMD. The only operation that is not  
401 directly applicable in HE is the division that we approximated with a Chebyshev polynomial. Note that we avoid any other  
402 division in the protocol by pushing them to the last step that is executed by the querier  $Q$  after decryption. In *Supplementary  
403 Protocol S2a*, we keep  $1/c$  until decryption.

404 In *Supplementary Protocol S2b*, we describe how we further reduce the computation overhead by obtaining the covariates'  
405 weights  $w'$  with a lightweight federated gradient-descent (FGD), by reporting the obtained covariates' contributions in the  
406 phenotype  $y$ , which becomes  $y''$ . To compute the p-value, we then compute only one element of the covariance inverse matrix  
407  $(X^T X')^{(-1)}[f+2; f+2]$ , instead of the entire inverse. To perform the federated gradient descent, we follow the method  
408 described by Froelicher et al.<sup>25</sup>, without disclosing any intermediate values.

409 We describe in *Supplementary Figure S3* how the (main) values used in both protocols are packed to optimize the  
410 communication and the amount of required operations (multiplications, rotations). We perform permutations, duplications, and  
411 rotations on cleartext data that are held by the DPs (indicated in orange in *Supplementary Figure S3*); and we avoid, as much as  
412 possible, the operations on encrypted vectors. Note that rotations on ciphertexts are almost two orders of magnitude slower than  
413 multiplications or additions and should be avoided when possible. As ciphertexts have to be aggregated among DPs, a tradeoff  
414 has to be found between computation cost (e.g., rotations) and data packing, as a smaller packing density would require the  
415 exchange of more ciphertexts.

416 In both protocols, all operations for  $v$  variants are executed in parallel, due to the ciphertext packing (SIMD). For a  
417 128-bit security level, the computations are performed simultaneously for 512 variants with FAMHE-GWAS and for 8192 with  
418 FAMHE-FastGWAS. These operations are further parallelized due to multi-threading and to the distribution of the workload  
419 among the DPs. We highlight (in bold) the main steps and aggregated values in the protocol and note that DPs' local data are in  
420 cleartext, whereas all exchanged data are collectively encrypted  $(E())$ .

421 **Baseline Computations with PLINK.** As explained in *Results*, we relied on the PLINK software to obtain our baseline  
422 results for the (i) *Original* approach in which GWAS is computed on the entire centralized dataset, (ii) the *Independent* approach  
423 in which each data provider performs the GWAS on its own subset of the data and (iii), for the *Meta-analysis* in which the data  
424 providers perform the GWAS on their local data before combining their results. For (i) and (ii), we relied on PLINK 2.0 and its  
425 linear regression (-glm option) based association test. For (iii), we relied on PLINK 1.9 and used the weighted-Z test approach  
426 to perform the meta-analysis.

## 427 **Experimental Settings**

428 We implemented our solution by building on top of Lattigo<sup>33</sup>, an open-source Go library for lattice-based cryptography, and  
429 on Onet, an open-source Go library for building decentralized systems. The communication between data providers (DPs) is  
430 done through TCP, with secure channels (by using TLS). We evaluate our prototype on an emulated realistic network, with  
431 a bandwidth of 1 Gbps and a delay of 20 ms between every two nodes. We deploy our solution on 12 Linux machines with  
432 Intel Xeon E5-2680 v3 CPUs running at 2.5GHz with 24 threads on 12 cores and 256 Gigabytes of RAM, on which we evenly  
433 distribute the DPs. We choose security parameters to always achieve a security level of 128 bits.

## 434 **Differentially Private Mechanism**

435 Differential privacy is a privacy-preserving approach, introduced by Dwork<sup>26</sup>, for reporting results on statistical datasets.  
436 This approach guarantees that a given randomized statistic,  $\mathcal{M}(DS) = R$ , computed on a dataset  $DS$ , behaves similarly when  
437 computed on a neighbor dataset  $DS'$  that differs from  $DS$  in exactly one element. More formally,  $(\epsilon, \delta)$ -differential privacy<sup>50</sup> is

438 defined by  $\Pr[\mathcal{M}(DS) = R] \leq \exp(\epsilon) \cdot \Pr[\mathcal{M}(DS') = R] + \delta$ , where  $\epsilon$  and  $\delta$  are privacy parameters: the closer to 0 they are,  
439 the higher the privacy level is.  $(\epsilon, \delta)$ -differential privacy is often achieved by adding noise to the output of a function  $f(DS)$ .  
440 This noise can be drawn from the Laplace distribution with mean 0 and scale  $\frac{\Delta f}{\epsilon}$ , where  $\Delta f$ , the sensitivity of the original real  
441 valued function  $f$ , is defined by  $\Delta f = \max_{D, D'} \|f(DS) - f(DS')\|_1$ . Other mechanisms, e.g., relying on a Gaussian distribution,  
442 were also proposed<sup>26,51</sup>.

443 As explained before, FAMHE can enable the participants to agree on a privacy level by choosing whether to yield exact or  
444 obfuscated, i.e., differentially private results, to the querier. We also note that our solution would then enable the obfuscation of  
445 only the final result, i.e., the noise can be added before the final decryption, and all the previous steps can be executed with  
446 exact values as no intermediate value is decrypted. This is a notable improvement with respect to existing federated-learning  
447 solutions, based on differential privacy<sup>38</sup>, in which the noise has to be added by each data provider at each iteration of the  
448 training. In the solution by Kim et al.<sup>38</sup>, each data provider perturbs its locally computed gradient such that the aggregated  
449 perturbation, obtained when the data providers aggregate (combine) their locally updated model, is  $\epsilon$ -differentially private. This  
450 is achieved by having each data provider generate and add a partial noise such that, when aggregated, the total noise follows  
451 the Laplace distribution. The noise magnitude is determined by the sensitivity of the computed function and this sensitivity is  
452 similar for each DP output and for the aggregated final result. This means that, as the intermediate values remain encrypted in  
453 FAMHE, a noise with the same magnitude can be added only once on the final result, thus ensuring the same level of privacy  
454 with a lower distortion of the result.

## 455 References

- 456 1. The EU General Data Protection Regulation. <https://eugdpr.org/>, (10.01.2021).
- 457 2. Sheller, M. J. *et al.* Federated Learning in Medicine: Facilitating Multi-institutional Collaborations without Sharing Patient  
458 Data. *Sci. reports* **10**, 1–12 (2020).
- 459 3. Nasirigerdeh, R. *et al.* sPLINK: A Federated, Privacy-Preserving Tool as a Robust Alternative to Meta-Analysis in  
460 Genome-Wide Association Studies. *BioRxiv* (2020).
- 461 4. Warnat-Herresthal, S. *et al.* Swarm Learning as a Privacy-preserving Machine Learning Approach for Disease Classification.  
462 *bioRxiv* (2020).
- 463 5. Zhu, L. & Han, S. Deep Leakage from Gradients. In *Federated Learning*, 17–31 (Springer, 2020).
- 464 6. Melis, L., Song, C., De Cristofaro, E. & Shmatikov, V. Exploiting Unintended Feature Leakage in Collaborative Learning.  
465 In *2019 IEEE Symposium on Security and Privacy (SP)*, 691–706 (IEEE, 2019).
- 466 7. Gaye, A. *et al.* DataSHIELD: Taking the Analysis to the Data, not the Data to the Analysis. *Int. journal epidemiology* **43**,  
467 1929–1944 (2014).
- 468 8. Moncada-Torres, A., Martin, F., Sieswerda, M., van Soest, J. & Geleijnse, G. VANTAGE6: an open source priVAcY  
469 preserviNg federaTed leArninG infrastructurE for Secure Insight eXchange. In *AMIA Annual Symposium Proceedings*,  
470 870–877 (2020).
- 471 9. All of Us Research Program, NIH. <https://allofus.nih.gov/>, 30.01.2021.
- 472 10. Genomics England. <https://www.genomicsengland.co.uk/>, 30.01.2021.
- 473 11. UK Biobank. <https://www.ukbiobank.ac.uk/>, 30.01.2021.
- 474 12. Scheibner, J. *et al.* Revolutionizing Medical Data Sharing Using Advanced Privacy Enhancing Technologies: Technical,  
475 Legal and Ethical Synthesis. *J Med Internet Res (in press)*. doi:10.2196/25120 (2021).
- 476 13. Wang, Z. *et al.* Beyond Inferring Class Representatives: User-Level Privacy Leakage From Federated Learning. In *IEEE  
477 INFOCOM* (2019).
- 478 14. Melis, L., Song, C., De Cristofaro, E. & Shmatikov, V. Exploiting Unintended Feature Leakage in Collaborative Learning.  
479 In *2019 IEEE Symposium on Security and Privacy (SP)* (2019).
- 480 15. Nasr, M., Shokri, R. & Houmansadr, A. Comprehensive Privacy Analysis of Deep Learning: Passive and Active White-box  
481 Inference Attacks against Centralized and Federated Learning. In *IEEE S&P* (2019).
- 482 16. Bonomi, L., Jiang, X. & Ohno-Machado, L. Protecting Patient Privacy in Survival Analyses. *J. Am. Med. Informatics  
483 Assoc.* **27**, 366–375 (2020).
- 484 17. Li, W. *et al.* Privacy-Preserving Federated Brain Tumour Segmentation. In *MLMI* (2019).

485 18. Jagadeesh, K. A., Wu, D. J., Birgmeier, J. A., Boneh, D. & Bejerano, G. Deriving Genomic Diagnoses without Revealing  
486 Patient Genomes. *Science* **357**, 692–695 (2017).

487 19. Cho, H., Wu, D. J. & Berger, B. Secure Genome-Wide Association Analysis using Multiparty Computation. *Nat. biotechnology* **36**, 547–551 (2018).

489 20. Hie, B., Cho, H. & Berger, B. Realizing private and practical pharmacological collaboration. *Science* **362**, 347–350 (2018).

490 21. Simmons, S., Sahinalp, C. & Berger, B. Enabling privacy-preserving gwass in heterogeneous human populations. *Cell systems* **3**, 54–61 (2016).

492 22. Froelicher, D. *et al.* Unlynx: A Decentralized System for Privacy-Conscious Data Sharing. *PETS* (2017).

493 23. Raisaro, J. L. *et al.* Medco: Enabling Secure and Privacy-Preserving Exploration of Distributed Clinical and Genomic  
494 Data. *IEEE/ACM Transactions on Comput. Biol. Bioinforma.* (2018).

495 24. Froelicher, D., Troncoso-Pastoriza, J. R., Sousa, J. S. & Hubaux, J. Drynx: Decentralized, Secure, Verifiable System for  
496 Statistical Queries and Machine Learning on Distributed Datasets. *IEEE TIFS* DOI: [10.1109/TIFS.2020.2976612](https://doi.org/10.1109/TIFS.2020.2976612) (2020).

497 25. Froelicher, D. *et al.* Scalable Privacy-Preserving Distributed Learning. *PETS* (2021).

498 26. Dwork, C., Roth, A. *et al.* The Algorithmic Foundations of Differential Privacy. *Foundations Trends Theor. Comput. Sci.*  
499 **9**, 211–407 (2014).

500 27. Jayaraman, B. & Evans, D. Evaluating Differentially Private Machine Learning in Practice. In *USENIX Security* (2019).

501 28. Raisaro, J. *et al.* SCOR: A Secure International Informatics Infrastructure to Investigate COVID-19. *J. Am. Med. Info. Assoc.* (2020).

503 29. Mouchet, C., Troncoso-pastoriza, J. R., Bossuat, J.-P. & Hubaux, J. P. Multiparty Homomorphic Encryption: From Theory  
504 to Practice. In *Tech. Report* <https://eprint.iacr.org/2020/304> (2019).

505 30. Samstein, R. M. *et al.* Tumor Mutational Load Predicts Survival after Immunotherapy across Multiple Cancer Types. *Nat. genetics* **51**, 202–206 (2019).

507 31. McLaren, P. J. *et al.* Polymorphisms of Large Effect Explain the Majority of the Host Genetic Contribution to Variation of  
508 HIV-1 Virus Load. *Proc. Natl. Acad. Sci.* **112**, 14658–14663 (2015).

509 32. iDash Competition. <http://www.humangenomeprivacy.org/2020/>, (11.01.2021).

510 33. Lattigo: A Library for Lattice-based Homomorphic Encryption in Go. <https://github.com/ldsec/lattigo>, 10.01.2021.

511 34. Tierney, J. F., Stewart, L. A., Ghersi, D., Burdett, S. & Sydes, M. R. Practical Methods for Incorporating Summary  
512 Time-to-event Data into Meta-analysis. *Trials* **8**, 16 (2007).

513 35. Laird, N. & Olivier, D. Covariance Analysis of Censored Survival Data using Log-linear Analysis Techniques. *J. Am. Stat. Assoc.* **76**, 231–240 (1981).

515 36. Plink Software. <https://www.cog-genomics.org/plink/>, 30.11.2020.

516 37. Lu, Y., Zhou, T., Tian, Y., Zhu, S. & Li, J. Web-Based Privacy-Preserving Multicenter Medical Data Analysis Tools Via  
517 Threshold Homomorphic Encryption: Design and Development Study. *J. medical Internet research* **22**, e22555 (2020).

518 38. Kim, M., Lee, J., Ohno-Machado, L. & Jiang, X. Secure and Differentially Private Logistic Regression for Horizontally  
519 Distributed Data. *IEEE Transactions on Inf. Forensics Secur.* **15**, 695–710 (2020).

520 39. Medco Software. <https://medco.epfl.ch/>, 10.01.2021.

521 40. Fan, J. & Vercauteren, F. Somewhat Practical Fully Homomorphic Encryption. *IACR Cryptol. ePrint Arch.* (2012).

522 41. Cheon, J. H., Kim, A., Kim, M. & Song, Y. Homomorphic Encryption for Arithmetic of Approximate Numbers. In  
523 *ASIACRYPT* (2017).

524 42. Lyubashevsky, V., Peikert, C. & Regev, O. On Ideal Lattices and Learning with Errors over Rings. In *EUROCRYPT* (2010).

525 43. Shamir, A. How to Share a Secret. *Commun. ACM* (1979).

526 44. Libert, B., Ling, S., Nguyen, K. & Wang, H. Lattice-based Zero-knowledge Arguments for Integer Relations. In *CRYPTO*  
527 (2018).

528 45. Sav, S. *et al.* POSEIDON: Privacy-Preserving Federated Neural Network Learning. *NDSS* (2021).

529 46. Atkinson, K. E. *An Introduction to Numerical Analysis* (John wiley & sons, 2008).

530 47. Goel, M. K., Khanna, P., & Kishore, J. Understanding Survival Analysis: Kaplan-Meier Estimate. *Int. journal Ayurveda research* (2010).

532 48. Sherman, J. & Morrison, W. J. Adjustment of an Inverse Matrix Corresponding to a Change in One Element of a Given Matrix. *The Annals Math. Stat.* **21**, 124–127 (1950).

534 49. WITDOM: empoWerIng prIvacy and securiTy in non-trusteD envirOnMents. <https://cordis.europa.eu/project/id/644371/> results, 30.01.2021.

536 50. Dwork, C., McSherry, F., Nissim, K. & Smith, A. Calibrating Noise to Sensitivity in Private Data Analysis. In *Theory of cryptography conference*, 265–284 (Springer, 2006).

538 51. Ghosh, A., Roughgarden, T. & Sundararajan, M. Universally Utility-maximizing Privacy Mechanisms. *SIAM J. on Comput.* **41**, 1673–1693 (2012).

540 52. Data Sharing Network (SHRINE). <https://www.i2b2.org/work/shrine.html>, (11.01.2021).

541 53. Han, K. & Ki, D. Better bootstrapping for approximate homomorphic encryption. In *CT-RSA* (2020).

## 542 Acknowledgements

543 We would like to thank Apostolos Pyrgelis for providing valuable feedback. This work was partially supported by the grant  
544 #2017-201 of the Strategic Focal Area “Personalized Health and Related Technologies (PHRT)” of the ETH Domain. This  
545 work was also partially supported by NIH R01 HG010959 (to B.B.) and NIH DP5 OD029574 (to H.C.).

## 546 Author Contributions Statement

547 J.R.T.-P, J.L.R. and J.P.H. conceived the study. D.F. and J.R.T.-P. developed the methods. D.F. and J.S.S. implemented the  
548 software and performed experiments, the results of which were validated by M.C. and J.F. H.C. and B.B. provided biological  
549 interpretation of the results and helped revise the manuscript. All authors contributed to the methodology and wrote the  
550 manuscript.

## 551 Data Availability

552 We replicated two existing medical studies, Samstein et al.<sup>30</sup> and McLaren et al.<sup>31</sup>, and we refer the reader to these works to  
553 obtain the related datasets.

## 554 Additional Information

555 The authors declare no competing financial interests.

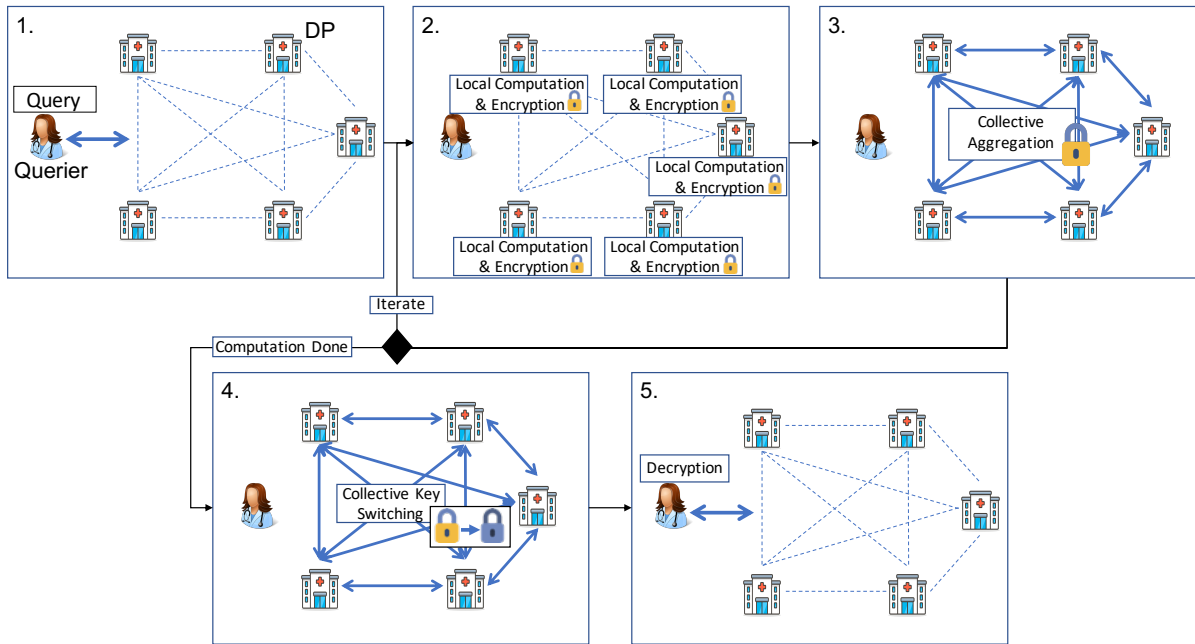


**Figure 1. System Model and FAMHE Workflow.** All entities are interconnected (dashed lines) and communication links at each step are shown by thick arrows. All entities (data providers (DPs) and querier) are honest-but-curious and do not trust each other. In **1.** the querier sends the query (in clear) to all the DPs who (**2.**) locally compute on their cleartext data and encrypt their results with the collective public key. In **3.** the DPs' encrypted local results are aggregated. For iterative tasks, this process is repeated (**Iterate**). In **4.** the final result is then collectively switched by the DPs from the collective public key to the public key of the querier. In **5.** the querier decrypts the final result.

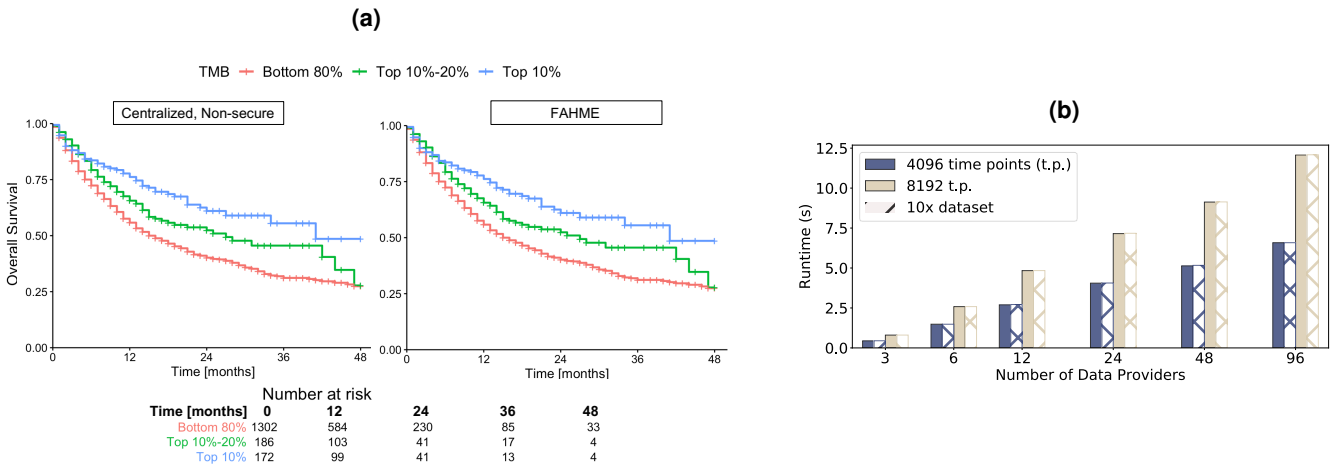


**Figure 2. Secure and Distributed Reproduction of a Survival-Curve Study.** (a): survival curves generated in a centralized non-secure manner and with FAMHE on the data used by Samstein et al.<sup>30</sup>. With FAMHE, the original data are split among three data providers, and the querier obtains exact results. The table in Figure a displays the number of patients at risk in a specific time. The exact same numbers are obtained with the centralized, non-secure solution and with FAMHE. (b): FAMHE execution time for the computation of one (or multiple) survival curve(s) with a maximum of 8192 time points. For both the aggregation and key switching (from the collective public key to the querier's key), most of the execution time is spent in communication (up to 98%), as the operations on the encrypted data are lightweight and parallelized on multiple levels, i.e., among the data providers and among the encrypted values.

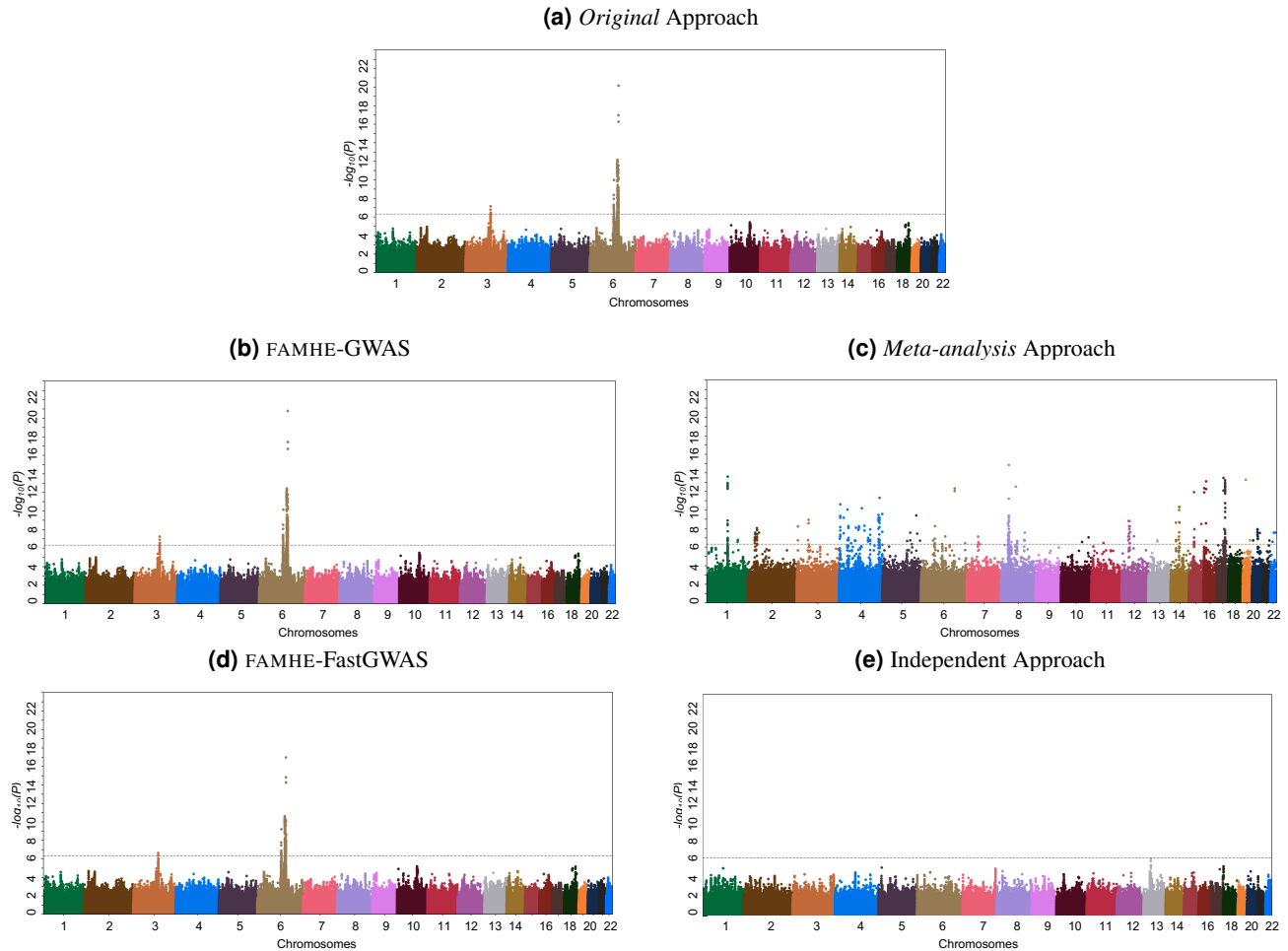


**Figure 3. Comparison of the GWAS results obtained with different approaches with 12 DPs (when applicable).** (a) Original is considered as the ground-truth and is obtained on a centralized cleartext dataset by relying on the PLINK<sup>36</sup> software. (c) and (e) are also obtained with PLINK (See *Online Methods* and *Supplementary* for complementary Figure S4). (b) and (d) are the results obtained with FAMHE-GWAS and FAMHE-FastGWAS, respectively. In the original study and in our secure approach, genome-wide signals of association ( $\log_{10}(P) < 5 \times 10^7$ , dotted line) were observed on chromosomes 6 and 3.

		Indep.		Meta-ana.		FAMHE-FastGWAS		FAMHE-GWAS	
		$-\log_{10}(\text{P-val})$	w	$-\log_{10}(\text{P-val})$	w	$-\log_{10}(\text{P-val})$	w	$-\log_{10}(\text{P-val})$	w
3 DPs	all	0.369	0.04	0.448	0.04	$6.7e^{-3}$	$1.5e^{-3}$	$2.72e^{-3}$	$7.3e^{-4}$
	peaks	4.14	0.055	7.9	0.19	0.71	$6.61e^{-3}$	0.1392	$1.88e^{-7}$
6 DPs	all	0.409	0.0665	0.45	0.041	$8.3e^{-3}$	$1.61e^{-3}$	$2.78e^{-3}$	$7.4e^{-4}$
	peaks	4.86	0.12	7.95	0.195	0.82	$6.63e^{-3}$	0.1393	$2.3e^{-7}$
12 DPs	all	0.425	0.104	0.453	0.048	$9e^{-3}$	$1.63e^{-3}$	$2.79e^{-3}$	$7.7e^{-4}$
	peaks	6.619	0.126	7.99	0.197	0.848	$6.69e^{-3}$	0.1399	$3.6e^{-7}$

**Table 1. Absolute averaged error on the logarithm of the p-values ( $-\log_{10}(\text{P-val})$ ) and on the model weights (w) between *Original* and federated approaches.** The Table also shows that one data provider performing the GWAS alone, with only its local data (**Indep.**), obtains inaccurate results. For each number of data providers, we report the error averaged over all positions and the errors on the peaks identified with *Original* (see Figure 3a).

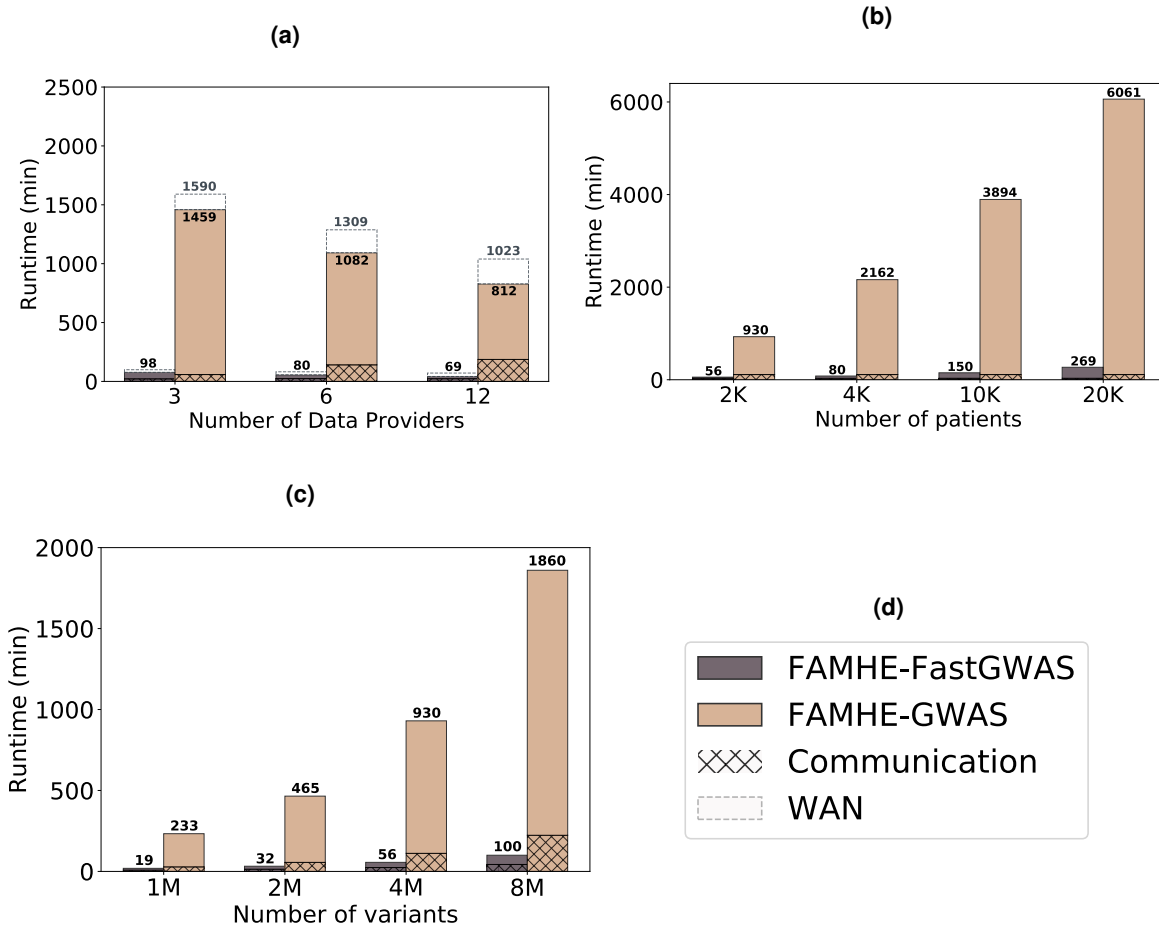


**Figure 4. FAMHE Scaling.** (a) FAMHE's scaling with the number of data providers, (b) with the size of the dataset and (c) with the number of variants considered in the GWAS. (d) is the legend box for (a, b, c). In (a), we also observe the effect of a reduced available bandwidth (from 1Gbps to 500Mbps) and increased communication delay (from 20ms to 40ms) on FAMHE's execution time. Unless otherwise stated, the original dataset containing 1857 samples and 4 million variants is evenly split among the data providers. By default, the number of DPs is fixed to 6.